

# Correlation among extinction efficiency and other parameters in an aggregate dust model

Tanuj Kumar Dhar and Himadri Sekhar Das

Department of Physics, Assam University, Silchar 788011, India; [hsdas13@gmail.com](mailto:hsdas13@gmail.com)

Received 2017 Feb XX; accepted 2017 XXXX

**Abstract** We study the extinction properties of highly porous BCCA dust aggregates in a wide range of complex refractive indices ( $1.4 \leq n \leq 2.0$ ,  $0.001 \leq k \leq 1.0$ ) and wavelength ( $0.11\mu m \leq \lambda \leq 3.4\mu m$ ). An attempt has been made for the first time to investigate the correlation among extinction efficiency ( $Q_{ext}$ ), the composition of dust aggregates ( $n, k$ ), the wavelength of radiation ( $\lambda$ ) and size parameter of the monomers ( $x$ ). If  $k$  is fixed at any value between 0.001 and 1.0,  $Q_{ext}$  increases with increase of  $n$  from 1.4 to 2.0.  $Q_{ext}$  and  $n$  are correlated via *linear* regression when the cluster size is small whereas the correlation is *quadratic* at moderate and higher sizes of the cluster. This feature is observed at all wavelengths (UV to optical to infrared). We also find that the variation of  $Q_{ext}$  with  $n$  is very small when  $\lambda$  is high. When  $n$  is fixed at any value between 1.4 and 2.0, it is observed that  $Q_{ext}$  and  $k$  are correlated via polynomial regression equation (of degree 1, 2, 3 or 4), where the degree of the equation depends on the cluster size,  $n$  and  $\lambda$ . The correlation is linear for small size and quadratic/cubic/quartic for moderate and higher sizes. We have also found that  $Q_{ext}$  and  $x$  are correlated via a polynomial regression (of degree 3,4 or 5) for all values of  $n$ . The degree of regression is found to be  $n$  and  $k$ -dependent. The set of relations obtained from our work can be used to model interstellar extinction for dust aggregates in a wide range of wavelengths and complex refractive indices.

**Key words:** Light scattering; ISM: dust, extinction.

## 1 INTRODUCTION

The studies of cometary and interplanetary dust indicate that cosmic dust grains are likely to be fluffy, porous and composites of many small grains fused together, due to dust-gas interactions, grain-grain collisions, and various other processes (Kruger and Kissel 1989; Greenberg & Hage 1990; Wolff et al. 1994). Porous, composite aggregates are often modelled as cluster of small spheres (known as “monomers”), agglomerated under various aggregation rules. Here grain aggregates are assumed to be fluffy sub structured

of a single material, such as silicates or carbon, as formed in the various separate sources of cosmic dust. Extinction generally takes place whenever electromagnetic radiation propagates through a medium containing small particles. The spectral dependence of extinction, or extinction curve, is a function of the structure, composition, and size distribution of the particles. The study of interstellar extinction provides us useful information for understanding the properties of the dust.

It is now well accepted from observation and laboratory analysis of interplanetary dust particles that cosmic dust grains are *fluffy aggregates* or *porous* with irregular shapes (Brownlee et al. 1985; Mathis and Whiffen 1989; Greenberg & Hage 1990). Using Discrete Dipole Approximation (DDA) technique, several investigators studied the extinction properties of the composite grains (Wolff et al. 1994, 1998; Voshchinnikov et al. 2006; Vaidya and Gupta 1999; Vaidya et al. 2007; Vaidya and Gupta 2009). Iati et al. (2004) studied optical properties of composite grains as grain aggregates of amorphous carbon and astronomical silicates, using the Superposition transition matrix approach. Recently, Mazarbhuiya and Das (2017) studied the light scattering properties of aggregate particles in a wide range of complex refractive indices and wavelengths to investigate the correlation among different parameters e.g., the positive polarization maximum, the amplitude of the negative polarization, geometric albedo, refractive indices and wavelength. The simulations were performed using the Superposition T-matrix code with Ballistic ClusterCluster Aggregate (BCCA) particles of 128 monomers and Ballistic Aggregates (BA) particles of 512 monomers.

The extinction efficiency of dust aggregates depends on aggregate size, composition and wavelength of incident radiation. The dependence of complex refractive index ( $n, k$ ) on  $Q_{ext}$  was studied by many groups in past for spherical and irregular particles using different scattering theories (Mie theory, DDA approach, T-matrix theory etc.). But no correlation equations were reported earlier by any group. In this paper, we study the extinction properties of randomly oriented porous dust aggregates with a wide range of complex refractive indices and wavelength of incident radiation. An attempt has been made for the first time to investigate the correlation among extinction efficiency ( $Q_{ext}$ ), complex refractive indices ( $m = n + ik$ ), wavelength ( $\lambda$ ) and the size parameter of monomer ( $x$ ).

## 2 NUMERICAL COMPUTATIONS

We have constructed the aggregates using ballistic aggregation procedure (Meakin 1983, 1984) using two different models of cluster growth. First via single-particle aggregation and then through cluster-cluster aggregation. These aggregates are built by random hitting and sticking particles together. The first one is called Ballistic Particle-Cluster Aggregate (BPCA) when the method allows only single particles to join the cluster of particles. If the method allows clusters of particles to stick together, the aggregate is called Ballistic Cluster-Cluster Aggregate (BCCA). Actually, the BPCA clusters are more compact than BCCA clusters (Mukai et al. 1992). The porosity of BPCA and BCCA particles of 128 monomers has the values 0.90 and 0.94, respectively. The fractal dimensions of BPCA and BCCA particles are given by  $D \approx 3$  and  $\approx 2$ , respectively (Meakin 1984). A systematic explanation on dust aggregate model is already discussed in our previous work (Das et al. 2008). It is to be noted that the structure of these aggregates are similar to

is also well understood from the laboratory diagnosis that the particle coagulation in the solar nebula grows under BCCA process (Wurm and Blum 1998).

The general extinction  $A_\lambda$  is given by (Spitzer 1978):

$$A_\lambda = -2.5 \log \left[ \frac{F(\lambda)}{F_0(\lambda)} \right] = 1.086 N_d Q_{ext} \sigma_d, \quad (1)$$

where  $F(\lambda)$  and  $F_0(\lambda)$  are the observed and expected fluxes,  $N_d$  is the dust column density,  $Q_{ext}$  is the extinction efficiency factor determined from Superposition T-matrix code, and  $\sigma_d$  is the geometrical cross-section of a single particle.

The interstellar extinction curve (i.e. the variation of extinction with wavelength) is usually expressed by the ratio  $A_\lambda/E(B-V)$  versus  $1/\lambda$ . The extinction curve covers the wavelength range 0.11 to 3.4  $\mu m$ . The entire range consists of UV (ultra violet), visible and IR (infrared) regions. The IR range corresponds to near infrared i.e. 0.750 to 2.5  $\mu m$ , the Visible range (0.38 to 0.76  $\mu m$ ) and the UV range (the last part of violet in visible spectrum to 0.11  $\mu m$ ).

The radius of an aggregate particle can be described by the radius of a sphere of equal volume given by  $a_v = a_m N^{1/3}$ , where  $N$  is the number of monomers in the aggregate and  $a_m$  is the monomer's radius of aggregates. We have found from literature survey that most of the work related to interstellar extinction considered a normal size range of 0.001 to 0.250 micron, with a size distribution (mainly MRN distribution) (Jones 1988, Whittet 2003, Vaidya et al. 2007, Das et al. 2010). They found an 'optimum' for the range of the cluster size generally used. The above size range of the monomer is more or less capable of evaluating average observed interstellar extinction curve. If we consider  $N = 64$  and  $a_m$  in the range 0.001 to 0.065 micron (with a step size of 0.004 micron), then  $a_v$  will be 0.004 to 0.26 micron. This size range is almost comparable to the size range used by other investigators.

We use JaSTA-2 (Second version of the Java Superposition T-matrix Application) (Halder & Das 2017), which is an upgraded version of JaSTA (Halder et al. 2014), to execute our computations which is based on Mackowski and Mishchenko (1996)'s Superposition T-matrix code. All versions of JaSTA are freely available to download from <http://ausastro.in/jasta.html>. The computations with the T-matrix code is fast and this technique gives rigorous solutions for randomly oriented ensembles of spheres. It is to be noted that the results obtained from the Discrete Dipole Approximation (DDA) approach and the T-matrix approach are almost same. Kimura et al. (2001) showed the results with aggregates using the DDA and the T-matrix code, and found almost same results with both the code. We perform the computations with a wide range of complex refractive indices ( $n = 1.4, 1.5, 1.6, 1.7, 1.8, 1.9, 2.0$  and  $k = 0.001, 0.01, 0.05, 0.1, 0.3, 0.5, 0.7, 1.0$ ) and wavelengths (0.11, 0.12, 0.13, 0.16, 0.175, 0.185, 0.20, 0.207, 0.22, 0.23, 0.26, 0.30, 0.365, 0.40, 0.55, 0.6, 0.7, 0.8, 0.90 and 3.4  $\mu m$ ). In general, the range of  $n$  and  $k$  which is considered in our work almost covers the range of the complex refractive indices of silicate and carbon at different wavelengths. The numerical computation in the present work has been executed with BCCA cluster of 64 monomers.

We present the results for  $a_m = 0.001\mu m, 0.017\mu m, 0.041\mu m$  and  $0.065\mu m$  where  $a_v$  is given by  $0.004\mu m, 0.068\mu m, 0.16\mu m$  and  $0.26\mu m$ . The monomer size parameter ( $x = 2\pi a_m/\lambda$ ) is taken in a range from 0.01 to 1.6. This study is mainly concentrated on investigation of correlation among  $Q_{ext}$ ,  $(n, k)$ ,  $\lambda$ ,

### 3 RESULTS

#### 3.1 Dependence on monomer size ( $a_m$ )

##### 3.1.1 Correlation between $Q_{ext}$ and $n$

We perform the computations with a wide range of complex refractive indices ( $1.4 \leq n \leq 2.0$  and  $0.001 \leq k \leq 1.0$ ) and wavelength of incident radiation ( $0.11 \leq \lambda \leq 3.4\mu m$ ). To study the dependence of  $n$  and  $k$  on the extinction efficiency ( $Q_{ext}$ ), we can either plot  $Q_{ext}$  versus  $k$  by keeping  $n$  fixed or plot  $Q_{ext}$  versus  $n$  by keeping  $k$  fixed. We first show the results for moderate size of the cluster, i.e., at  $a_v = 0.16\mu m$ . The results at other three sizes are also presented thereafter.

We plot  $Q_{ext}$  versus  $n$  at  $a_v = 0.16\mu m$ , for  $k = 0.001, 0.01, 0.1, 0.5$  and  $1.0$  respectively (although we have executed the code with all eight values of  $k$  mentioned above), in a single frame, for  $\lambda = 0.11, 0.20, 0.30$  and  $0.90\mu m$ , which is shown in Fig.1. It is to be noted that the plots are shown for four wavelengths although the computations have been performed for all the wavelengths.

It is observed from Fig.1 that if  $k$  is fixed at any value between  $0.001$  and  $1.0$ ,  $Q_{ext}$  increases with increase of  $n$  from  $1.4$  to  $2.0$  at all wavelengths. But a small decrease in  $Q_{ext}$  is also noticed at  $\lambda = 0.11\mu m$  when  $n > 1.7$  and  $k$  is low. The variation of  $Q_{ext}$  with  $n$  is small when  $k \geq 0.5$ . The value of  $Q_{ext}$  is small when  $\lambda$  is large, i.e.  $Q_{ext}$  decreases when size parameter of the monomer ( $x = 2\pi a_m/\lambda$ ) decreases. We have also investigated that the variation of  $Q_{ext}$  with  $n$  is very small when  $\lambda \geq 0.70\mu m$ .

We have found that  $Q_{ext}$  and  $n$  can be fitted by *quadratic regression* where *coefficient of determination*<sup>1</sup> ( $R^2$ ) for each equation is  $\approx 0.99$ . The best fit equation is given by

$$Q_{ext} = A_k n^2 + B_k n + C_k \quad , \quad 1.4 \leq n \leq 2.0, \quad 0.001 \leq k \leq 1, \quad (2)$$

where,  $A_k, B_k$  and  $C_k$  are  $k$ -dependent coefficients of equation (2).

The coefficients obtained for different values of  $k$  (only five values of  $k$  are shown) are depicted in Table-1. If we plot coefficients  $A_k, B_k$  and  $C_k$  versus  $k$  (where  $k = 0.001, 0.01, 0.05, 0.1, 0.3, 0.5, 0.7, 1.0$ ), we find that the best fit curves correspond to *cubic regression*, which have  $R^2 \approx 0.99$ . We do not show any figures in this case.

The coefficients are correlated with  $k$  by the relations:

$$A_k = D_1 k^3 + D_2 k^2 + D_3 k + D_4 \quad , \quad (2a)$$

$$B_k = E_1 k^3 + E_2 k^2 + E_3 k + E_4 \quad , \quad (2b)$$

$$C_k = F_1 k^3 + F_2 k^2 + F_3 k + F_4 \quad , \quad (2c)$$

All coefficients of equation 2(a-c) are shown in Table-2. Thus knowing the coefficients, the extinction efficiency ( $Q_{ext}$ ) can be calculated for any value of  $n$  and  $k$  from the equation (2).

In Fig.2, we report the results for  $a_v = 0.004\mu m$  at  $\lambda = 0.11, 0.20, 0.30$  and  $0.90 \mu m$ . A strong *linear* correlation between  $Q_{ext}$  and  $n$  is seen at this size for all wavelengths from  $0.11$  to  $3.4 \mu m$ . In Fig.3, we plot  $Q_{ext}$  versus  $n$  for  $a_v = 0.068\mu m$  at  $\lambda = 0.11\mu m$  and  $0.60 \mu m$ . We have found that the nature is *quadratic*

<sup>1</sup> The *coefficient of determination* is a key output of regression analysis which is interpreted as the proportion of the variance in the

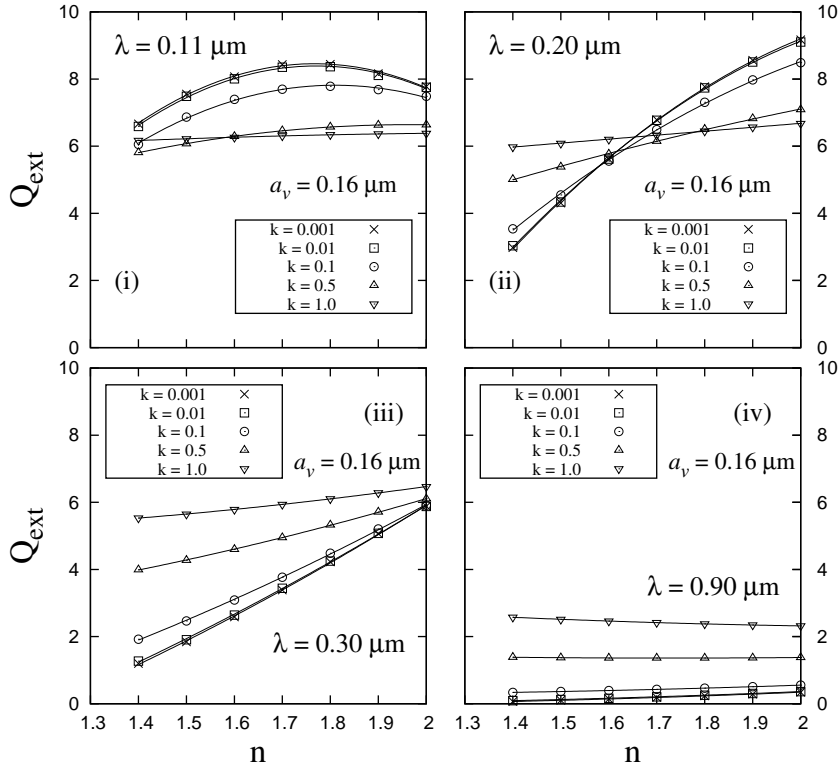


**Fig. 1** Extinction efficiency ( $Q_{ext}$ ) is plotted against real part of the refractive index ( $n$ ) for  $k = 0.001, 0.01, 0.1, 0.5$  and  $1.0$  at  $a_v = 0.16\mu m$ . The best fit curves correspond to *quadratic regression* of the form  $Q_{ext} = A_k n^2 + B_k n + C_k$  for wavelengths (i)  $0.11\mu m$ , (ii)  $0.20\mu m$ , (iii)  $0.30\mu m$  and (iv)  $0.90\mu m$ .

at all wavelengths from  $0.11$  to  $3.4\mu m$ . Finally, we show the results for  $a_v = 0.26\mu m$  at  $\lambda = 0.11\mu m$  and  $0.60\mu m$ , shown in Fig.4. We have noticed that the  $Q_{ext}$  and  $n$  is correlated via a *cubic regression* at  $0.11\mu m$  whereas the dependence is *quadratic* at other higher wavelengths. We do not show any equation or table in the above three cases. In summary, we can conclude that the correlation between  $Q_{ext}$  and  $n$  is *linear* when the cluster size is small whereas the correlation is *quadratic* at moderate and higher sizes of cluster.

### 3.1.2 Correlation between $Q_{ext}$ and $k$

We now plot  $Q_{ext}$  versus  $k$  for  $n = 1.4, 1.5, 1.6, 1.7, 1.8, 1.9$  and  $2.0$  respectively, at  $a_v = 0.16\mu m$  where  $\lambda$  is taken in between  $0.11\mu m$  and  $3.4\mu m$ . When  $\lambda$  is between  $0.11\mu m$  and  $0.26\mu m$ , we have found that  $Q_{ext}$  and  $k$  can be fitted via a polynomial regression equation where the degree of equation depends on the value of  $n$  and  $\lambda$ . In Fig.5 we show the plots for  $\lambda = 0.11, 0.16, 0.20$  and  $0.26\mu m$ . At  $\lambda = 0.11\mu m$ , we find that  $Q_{ext}$  and  $k$  are correlated by (i) *quartic regression* when  $n = 1.4$ , (ii) *cubic regression* when  $n = 1.5$

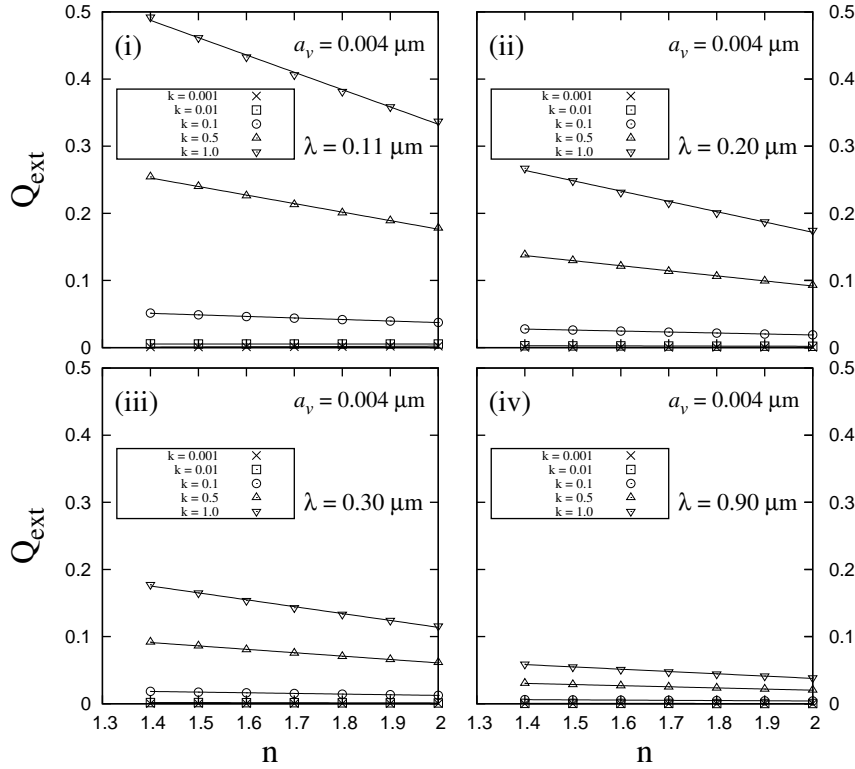


**Fig. 2** Extinction efficiency ( $Q_{ext}$ ) is plotted against real part of the refractive index ( $n$ ) for  $k = 0.001, 0.01, 0.1, 0.5$  and  $1.0$  at  $a_v = 0.004\mu m$ . The best fit curves correspond to *linear regression* for wavelengths (i)  $0.11\mu m$ , (ii)  $0.20\mu m$ , (iii)  $0.30\mu m$  and (iv)  $0.90\mu m$ .

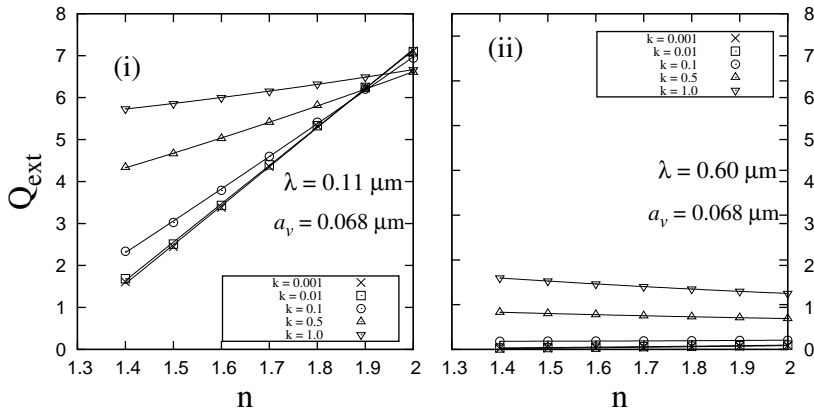


**Fig. 3** Extinction efficiency ( $Q_{ext}$ ) is plotted against real part of the refractive index ( $n$ ) for  $k = 0.001, 0.01, 0.1, 0.5$  and  $1.0$  at  $a_v = 0.068\mu m$ . The best fit curves correspond to *quadratic regression* for wavelengths (i)  $0.11\mu m$  and (ii)  $0.60\mu m$ .

**Table 1** Co-efficients of equation (2) are shown for  $\lambda = 0.11, 0.20, 0.30$  and  $0.90\mu m$ .

$\lambda$	$k$	$A_k$	$B_k$	$C_k$
0.11 $\mu m$	0.001	-13.245	46.876	-33.026
	0.01	-12.937	45.862	-32.263
	0.1	-10.123	36.537	-25.149
	0.5	-2.651	10.490	-3.731
	1.0	-0.346	1.555	4.661
0.20 $\mu m$	0.001	-7.815	36.995	-33.540
	0.01	-7.572	35.969	-32.527
	0.1	-5.439	26.899	-23.511
	0.5	-0.969	6.779	-2.590
	1.0	0.010	1.141	4.359
0.30 $\mu m$	0.001	1.651	2.290	-5.271
	0.01	1.647	2.191	-5.054
	0.1	1.589	1.335	-3.095
	0.5	3.527	-0.999	3.939
	1.0	0.681	-0.749	5.243
0.90 $\mu m$	0.001	0.217	-0.278	0.032
	0.01	0.217	-0.285	0.068
	0.1	0.213	-0.363	0.429
	0.5	0.230	-0.794	2.046
	1.0	0.328	-1.543	4.092

**Table 2** Co-efficients of equation 2(a-c) at  $\lambda = 0.11, 0.20, 0.30$  and  $0.90 \mu m$ .

		Coeff-1	Coeff-2	Coeff-3	Coeff-4
$\lambda = 0.11\mu m$	$A_k$	10.161	-31.889	34.662	-13.280
	$B_k$	-26.328	94.623	-113.730	46.990
	$C_k$	11.321	-58.956	85.407	-33.111
$\lambda = 0.20\mu m$	$A_k$	15.474	-35.001	27.379	-7.842
	$B_k$	-60.269	139.790	-115.490	37.110
	$C_k$	55.593	-131.620	114.040	-33.654
$\lambda = 0.30\mu m$	$A_k$	1.586	-2.127	-0.431	1.652
	$B_k$	-8.473	16.673	-11.251	2.302
	$C_k$	10.310	-24.081	24.309	-5.295
$\lambda = 0.90\mu m$	$A_k$	0.001	0.171	-0.060	0.217
	$B_k$	-0.024	-0.430	-0.812	-0.277
	$C_k$	0.002	0.053	4.009	0.028

*cubic* when  $n = 1.5, 1.6, 1.7$  &  $1.8$  and *quadratic* when  $n = 1.4, 1.9$  &  $2.0$ . The correlation at  $\lambda = 0.20\mu m$  is *cubic* when  $n = 1.6, 1.7$  &  $1.8$  and *quadratic* when  $n = 1.4, 1.5, 1.9$  &  $2.0$ . We also note that the correlation at  $0.26 \mu m$  is *quadratic* when  $n = 1.4, 1.5, 1.6, 1.7$  &  $1.8$  and *cubic* when  $n = 1.9$  &  $2.0$ . At low values of  $n$ ,  $Q_{ext}$  increases with increase of  $k$  whereas the trend is exactly opposite when  $n$  is high, e.g., at  $\lambda = 0.20\mu m$ ,  $Q_{ext}$  increases with  $k$  when  $n \leq 1.6$ , but it decreases when  $n \geq 1.7$ . The vertical range of  $Q_{ext}$  in the plot also decreases when  $k$  increases. This range is maximum at  $k = 0.001$  and minimum at  $k = 1.0$ .

In Fig.6, we show the plots for  $0.30 \leq \lambda \leq 3.4\mu m$  and we have found that the fit is *quadratic* for all

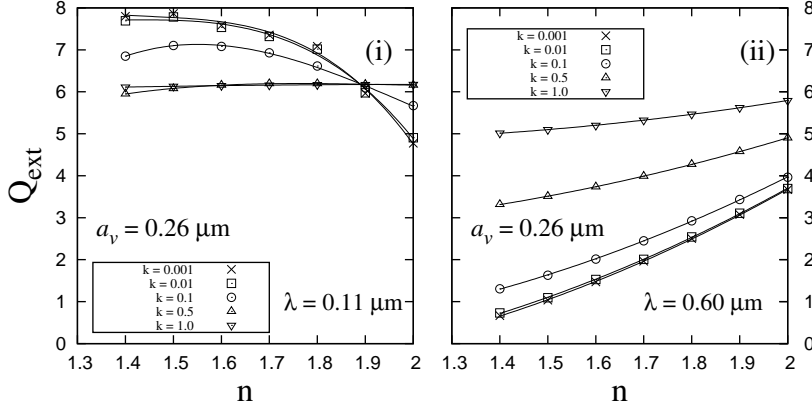


**Fig. 4** Extinction efficiency ( $Q_{ext}$ ) is plotted against real part of the refractive index ( $n$ ) for  $k = 0.001, 0.01, 0.1, 0.5$  and  $1.0$  at  $a_v = 0.26\mu m$ . The best fit curves correspond to *cubic regression* at (i)  $\lambda = 0.11\mu m$  and *quadratic regression* at (ii)  $\lambda = 0.60\mu m$ .

also decreases when  $k$  increases. Further, the plot of  $Q_{ext}$  with  $k$  is same at all values of  $n$  when  $\lambda$  is high (please see Fig.6(iv)).

The best fit equation in the wavelength range  $0.30\mu m$  to  $3.4\mu m$  is given by

$$Q_{ext} = A_n k^2 + B_n k + C_n, \quad 1.4 \leq n \leq 2.0, \quad 0.001 \leq k \leq 1 \quad (3)$$

where,  $A_n, B_n$  and  $C_n$  are  $n$ -dependent coefficients of equation (3).

The coefficients obtained for different values of  $k$  are shown in Table-3. If we plot coefficients  $A_n, B_n$  and  $C_n$  versus  $n$  (figures are not shown), we note that the best fit curves correspond to *quadratic regression*, which have  $R^2 \approx 0.99$ .

Thus coefficients are given by

$$A_n = D'_1 k^2 + D'_2 k + D'_3, \quad (3a)$$

$$B_n = E'_1 k^2 + E'_2 k + E'_3, \quad (3b)$$

$$C_n = F'_1 k^2 + F'_2 k + F'_3, \quad (3c)$$

All coefficients of equation 3(a-c) are shown in Table-4. Thus, knowing the coefficients of equation 3(a-c), the extinction efficiency ( $Q_{ext}$ ) can be also estimated for any value of  $n$  and  $k$  from the equation (3).

In Fig.7, we plot  $Q_{ext}$  against  $k$  for  $a_v = 0.004\mu m$  at  $\lambda = 0.11, 0.30, 0.60$  and  $0.90\mu m$ , although the computations have been performed for wide range of wavelengths from  $0.11$  to  $3.4\mu m$ . We observe the *linear* dependence at this size for all wavelengths. This linear nature becomes *quadratic* when the size of cluster is  $a_v = 0.068\mu m$ . Fig.8 shows the results for  $a_v = 0.068\mu m$  at  $\lambda = 0.11\mu m$  and  $0.60\mu m$ . In Fig.9, the results obtained for  $a_v = 0.26\mu m$  are plotted. In this case, the nature of dependence looks similar with  $a_v = 0.16\mu m$ .  $Q_{ext}$  and  $k$  are correlated via polynomial regression equation (of degree 2, 3 or 4) where the degree of equation depends on the real part of the refractive index ( $n$ ) at ( $\lambda = 0.11\mu m$ ) (please see caption of Fig.9). The nature is quadratic when  $\lambda > 0.11\mu m$ . In summary, we can conclude that the dependence of  $Q_{ext}$  on  $k$  depends on the cluster size. The correlation is linear for small size and quadratic/cubic for



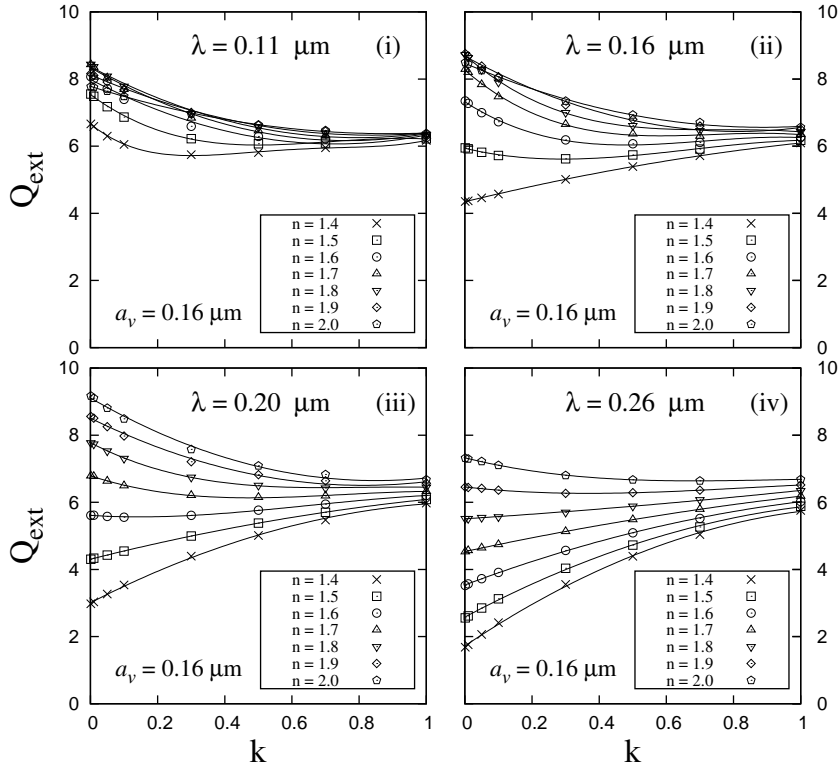


**Fig. 5** Extinction efficiency ( $Q_{ext}$ ) is plotted against imaginary part of the refractive index ( $k$ ) at  $\lambda = 0.11, 0.16, 0.20$  and  $0.26 \mu m$  at  $a_v = 0.16 \mu m$ . The best fit curves correspond to polynomial regression equation where the degree of equation depends on the value of  $n$  and  $\lambda$  (please see Section 3.2 for details).

It is important to mention that the real part of the complex index of refraction ( $n$ ) controls the effective phase speed of electromagnetic waves propagating through the medium, while the imaginary part  $k$  describes the rate of absorption of the wave. In any material,  $n$  and  $k$  are not free to vary independently of one another but rather are tightly coupled to one another via the so-called Kramer-Kronig relations. Therefore, the results presented above are quite expectable.

### 3.2 Dependence on wavelength of radiation ( $\lambda$ )

We now study the dependence of  $Q_{ext}$  on  $\lambda$  for a particular set of  $(n, k)$  in case of  $a_v = 0.16 \mu m$  only. We observe the following results:

- (i) For  $n = 1.4, 1.5$  and  $1.6$ ,  $Q_{ext}$  versus  $\lambda$  can be fitted via a *quartic* regression for  $k = 0.001, 0.01, 0.05, 0.1, 0.3, 0.5, 0.7$  and  $1.0$  (please see Fig.10).
- (ii) For  $n = 1.7, 1.8, 1.9$  and  $2.0$ ,  $Q_{ext}$  versus  $\lambda$  can be fitted via a *quartic* regression in the wavelength range  $0.11 - 0.40 \mu m$  [Fig.11(i,iv) and Fig.12(i,iv)] and a *quadratic* regression in the wavelength range

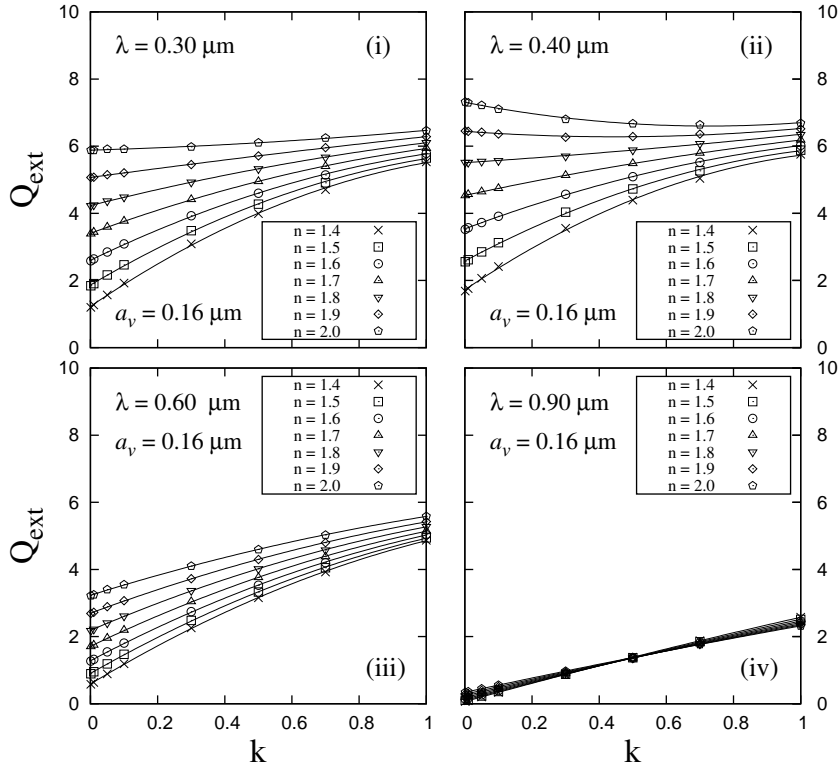


**Fig. 6** Extinction efficiency ( $Q_{ext}$ ) is plotted against imaginary part of the refractive index ( $k$ ) for  $n = 1.4, 1.5, 1.6, 1.7, 1.8, 1.9$  and  $2.0$  at  $a_v = 0.16\mu m$ . The best fit curves correspond to *quadratic regression* of the form  $Q_{ext} = A'_n k^2 + B'_n k + C'_n$  for wavelengths (i)  $0.30\mu m$ , (ii)  $0.40\mu m$ , (iii)  $0.60\mu m$  and (iv)  $0.90\mu m$ .

$\lambda$  can be fitted via a *quartic regression* in the wavelength range  $0.11 - 0.90\mu m$  for higher values of  $k = 0.5, 0.7$  and  $1$  [Fig. 11(iii,vi) and Fig. 12(iii,vi)]. We did not include the plots for  $\lambda = 3.4\mu m$ .

It is noticed from Figs. 10, 11 and 12 that  $Q_{ext}$  decreases with increase of  $\lambda$  when  $n \leq 1.6$ . When  $n \geq 1.7$ ,  $Q_{ext}$  initially increases with increase of  $\lambda$  and reaches a maximum value, then it starts decreasing if  $\lambda$  is increased further. We also observe that  $Q_{ext}$  is maximum at  $k = 0.001$  and minimum at  $k = 1.0$  when  $\lambda = 0.11\mu m$ . But this trend changes at a critical value of wavelength ( $\lambda_c$ ) where exactly opposite nature is noticed. We notice that  $\lambda_c$  is (i)  $0.16\mu m$  at  $n = 1.4$ , (ii)  $0.185\mu m$  at  $n = 1.5$ , (iii)  $0.207\mu m$  at  $n = 1.6$ , (iv)  $0.22\mu m$  at  $n = 1.7$ , (v)  $0.26\mu m$  at  $n = 1.8$ , (vi)  $0.26\mu m$  at  $n = 1.9$  and (vii)  $0.30\mu m$  at  $n = 1.4$ . The values of  $Q_{ext}$  is maximum at  $k = 1.0$  when  $\lambda > \lambda_c$ . We do not show any equations and tables in this case.

### 3.3 Dependence on the size parameter of monomer ( $x$ )

We now study the dependence of  $Q_{ext}$  on the size parameter of monomer ( $x = 2\pi a_m/\lambda$ ) for  $n = 1.4, 1.5,$

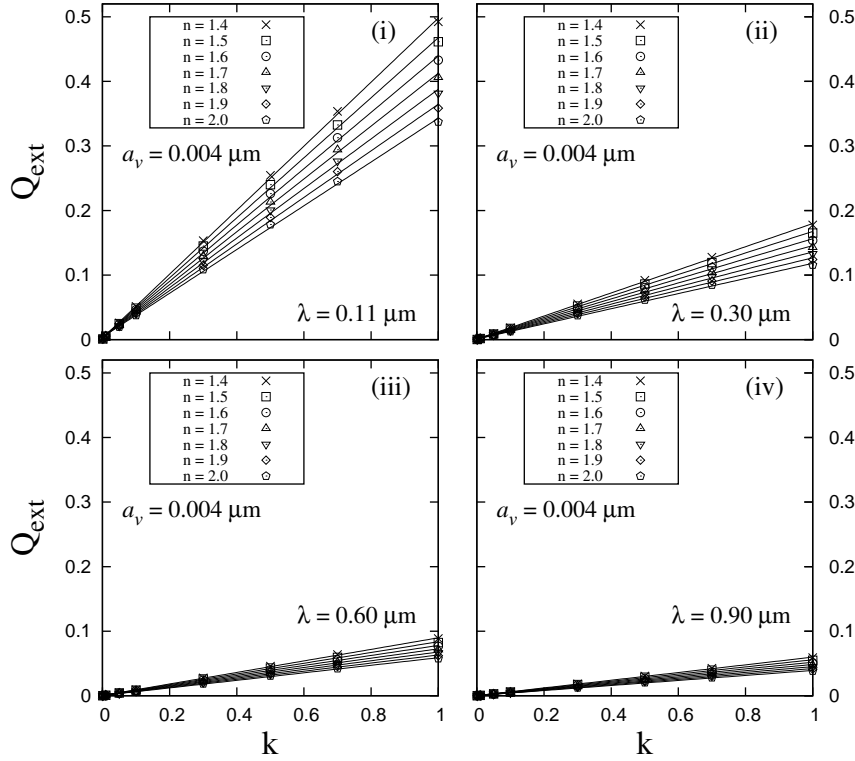


**Fig. 7** Extinction efficiency ( $Q_{ext}$ ) is plotted against imaginary part of the refractive index ( $k$ ) for  $n = 1.4, 1.5, 1.6, 1.7, 1.8, 1.9$  and  $2.0$  at  $a_v = 0.004 \mu m$ . The best fit curves correspond to *linear regression* for wavelengths (i)  $0.11 \mu m$ , (ii)  $0.30 \mu m$ , (iii)  $0.60 \mu m$  and (iv)  $0.90 \mu m$ .

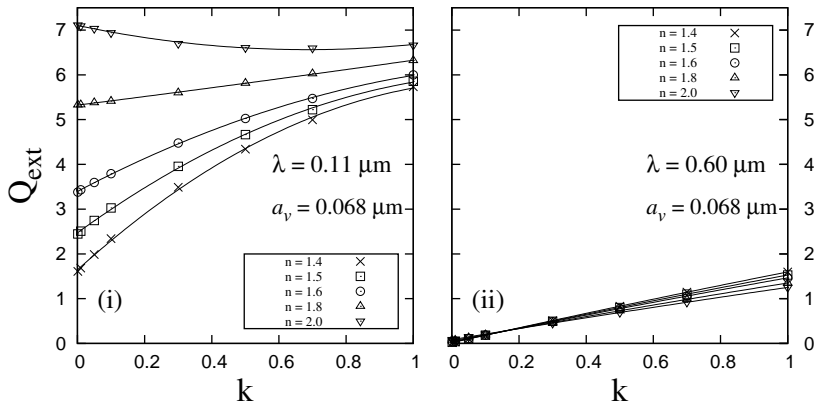


**Fig. 8** Extinction efficiency ( $Q_{ext}$ ) is plotted against imaginary part of the refractive index ( $k$ ) for  $n = 1.4, 1.5, 1.6, 1.8$  and  $2.0$  at  $a_v = 0.068 \mu m$ . The best fit curves correspond to *quadratic regression* for wavelengths (i)  $0.11 \mu m$  and (ii)  $0.60 \mu m$ .

**Table 3** Co-efficients of equation (3) at  $\lambda = 0.30, 0.40, 0.60$  and  $0.90 \mu m$ .

$\lambda$	$n$	$A_n$	$B_n$	$C_n$
0.30 $\mu m$	1.4	-2.579	6.890	1.195
	1.5	-2.107	5.844	1.896
	1.6	-1.630	4.774	2.632
	1.7	-1.148	3.678	3.401
	1.8	-0.661	2.556	4.204
	1.9	-0.169	1.410	5.041
	2.0	0.327	0.238	5.911
0.40 $\mu m$	1.4	-1.769	6.047	0.579
	1.5	-1.655	5.675	0.912
	1.6	-1.519	5.256	1.290
	1.7	-1.362	4.789	1.712
	1.8	-1.184	4.274	2.178
	1.9	-0.984	3.712	2.688
	2.0	-0.763	3.102	3.242
0.60 $\mu m$	1.4	-0.727	4.222	0.198
	1.5	-0.704	4.081	0.307
	1.6	-0.676	3.931	0.433
	1.7	-0.642	3.771	0.574
	1.8	-0.602	3.602	0.731
	1.9	-0.556	3.423	0.905
	2.0	-0.505	3.234	1.094
0.90 $\mu m$	1.4	-0.260	2.771	0.064
	1.5	-0.257	2.674	0.100
	1.6	-0.250	2.575	0.139
	1.7	-0.240	2.475	0.183
	1.8	-0.227	2.374	0.231
	1.9	-0.210	2.272	0.284
	2.0	-0.190	2.169	0.341

$0.01 \leq x \leq 1.6$  (where,  $N = 64$ ), is considered to investigate the correlation between  $Q_{ext}$  and  $x$ . The results are plotted in Figs. 13, 14, 15 and 16 for  $k = 0.001, 0.01, 0.1$  and  $1.0$ , respectively. It can be seen from figures that if  $x$  is fixed at any value between  $0.01$  and  $1.6$ ,  $Q_{ext}$  increases with increase of  $n$ . This increase is prominent when  $x > 0.2$ . The vertical range of  $Q_{ext}$  also increases with increase of  $n$  from  $1.4$  to  $2.0$ . This range is maximum (i) at  $x = 1.4$  in case of  $k = 0.001$  (where,  $Q_{ext} = [9.34, 3.45]$ ), (ii) at  $x = 1.4$  in case of  $k = 0.01$  (where,  $Q_{ext} = [9.26, 3.50]$ ), (iii) at  $x = 1.4$  in case of  $k = 0.1$  (where,  $Q_{ext} = [8.56, 3.90]$ ), and (iv) at  $x = 1.12$  in case of  $k = 1.0$  (where,  $Q_{ext}(\max) = [6.74, 5.88]$ ). The slope of  $Q_{ext}$  versus  $x$  curve increases with the increase of  $n$  from  $1.4$  to  $2.0$  which is noted for all values of  $k$ . It is also interesting to notice that the vertical range of  $Q_{ext}$  at  $x = 1.6$  decreases with the increase of  $k$  and is lowest at  $k = 1.0$ . Further,  $Q_{ext}$  value does not depend much on  $n$  for highly absorptive particles ( $k = 1.0$ ) when  $x < 0.5$ . The variation is also small when  $x > 0.5$ .

We have found that  $Q_{ext}$  and  $x$  can be fitted by a *cubic regression* for all values of  $n$  except  $2.0$ , in case

**Table 4** Co-efficients of equation 3(a-c) at  $\lambda = 0.30, 0.40, 0.60$  and  $0.90 \mu m$ .

$\lambda$		Coeff-1	Coeff-2	Coeff-3
0.30 $\mu m$	$A_n$	0.243	4.016	-8.679
	$B_n$	-1.269	-6.771	18.857
	$C_n$	1.682	2.142	-5.101
0.40 $\mu m$	$A_n$	1.069	-1.956	-1.126
	$B_n$	-2.385	3.201	6.241
	$C_n$	2.202	-3.048	0.530
0.60 $\mu m$	$A_n$	0.290	-0.614	-0.434
	$B_n$	-0.481	-0.010	5.179
	$C_n$	0.796	-1.214	0.337
0.90 $\mu m$	$A_n$	0.171	-0.466	0.056
	$B_n$	-0.060	-0.799	4.008
	$C_n$	0.217	-0.278	0.028

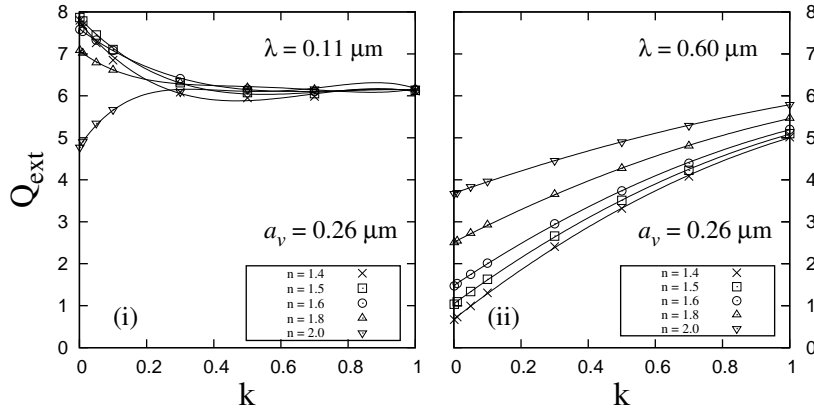


**Fig. 9** Extinction efficiency ( $Q_{ext}$ ) is plotted against imaginary part of the refractive index ( $k$ ) for  $n = 1.4, 1.5, 1.6, 1.8$  and  $2.0$  at  $a_v = 0.26 \mu m$ .  $Q_{ext}$  and  $k$  are correlated via polynomial regression equations, where the degree of regression is found to be wavelength dependent: (i) at  $\lambda = 0.11 \mu m$ , the correlation is *cubic* for  $n = 1.4, 1.5, 1.6, 1.7$  and  $2.0$ , and *quartic* at  $n = 1.8$  and  $1.9$ , and (ii) at  $\lambda = 0.60 \mu m$ , the correlation is *quadratic* at all values of  $n$ .

The best fit equation is given by

$$Q_{ext} = \alpha_1 x^3 + \alpha_2 x^2 + \alpha_3 x + \alpha_4, \quad (4)$$

where,  $\alpha_1, \alpha_2, \alpha_3$  and  $\alpha_4$  are  $n$ -dependent coefficients of equation (4). The coefficients are presented in Table-5.

However, the best fit equation in case of  $n = 2.0$  corresponds to a *quartic regression* for  $k = 0.001, 0.01$ , and  $0.1$ , which is given by

$$Q_{ext} = \beta_1 x^4 + \beta_2 x^3 + \beta_3 x^2 + \beta_4 x + \beta_5, \quad (5)$$

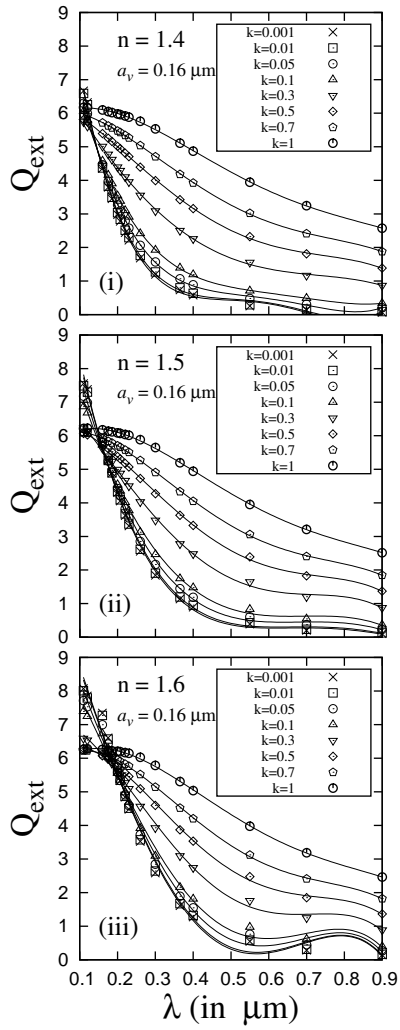


**Fig. 10** Extinction efficiency ( $Q_{ext}$ ) is plotted against wavelength ( $\lambda$ ) for  $k = 0.001, 0.01, 0.05, 0.1, 0.3, 0.5, 0.7$  and  $1.0$  at  $a_v = 0.16\mu\text{m}$  when (i)  $n = 1.4$ , (ii)  $n = 1.5$  and (iii)  $n = 1.6$ . The best fit curves correspond to *quartic regression*.

The correlation between  $Q_{ext}$  and  $x$  is found to be *quintic regression* for all values of  $n$  at  $k = 1.0$ . The best fit equation is given by

$$Q_{ext} = \gamma_1 x^5 + \gamma_2 x^4 + \gamma_3 x^3 + \gamma_4 x^2 + \gamma_5 x + \gamma_6, \quad (6)$$

where,  $\gamma_1, \gamma_2, \gamma_3, \gamma_4, \gamma_5,$  and  $\gamma_6$  are  $n$ -dependent constants of equation (6). The constants are given in Table-5.

Equations (4), (5) and (6) are very useful in estimating  $Q_{ext}$ , where one can generate a large data set for

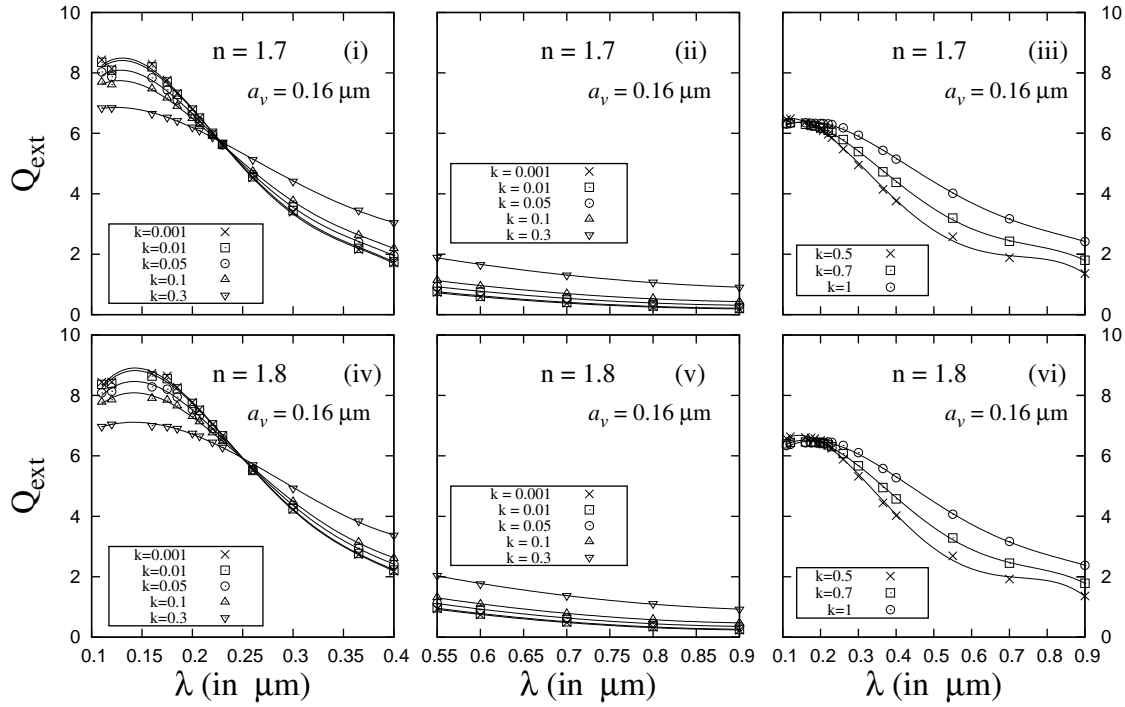


**Fig. 11** Extinction efficiency ( $Q_{ext}$ ) is plotted against wavelength of incident radiation ( $\lambda$ ) at  $a_v = 0.16 \mu\text{m}$ . The left panel (top and bottom) shows the plot for imaginary part of the refractive indices ( $k$ ) = 0.001, 0.01, 0.05, 0.1 & 0.3 in the wavelength range  $0.11 \mu\text{m}$  to  $0.40 \mu\text{m}$ , the middle panel (top and bottom) is for  $k = 0.001, 0.01, 0.05, 0.1$  &  $0.3$  in the wavelength range  $0.55 \mu\text{m}$  to  $0.90 \mu\text{m}$  and the right panel (top and bottom) is for  $k = 0.5, 0.7$  &  $1$  in the wavelength range  $0.11 \mu\text{m}$  to  $0.90 \mu\text{m}$ . The best fit corresponds to *quartic* regression (left panel), *quadratic* regression (middle panel) and *quartic* regression (right panel). The real part of the refractive index ( $n$ ) is fixed at 1.7 and 1.8.

#### 4 RESULTS FROM CORRELATION EQUATIONS

In the previous sections, we have obtained a set of correlation equations which can be used to calculate the extinction efficiency of dust aggregates with a wide range of size of aggregates and wavelength of radiation. We first calculate  $Q_{ext}$  from relations (2) and (3) for BCCA particles with  $N = 64$  and  $a_m = 0.041 \mu\text{m}$ , for selected values of  $n$ ,  $k$  and  $\lambda$ . The calculated values are compared with the computed values obtained using the Superposition T-matrix code. The results are shown in Table-6 and 7. We also estimate  $Q_{ext}$  using relations (4), (5) and (6) for selected values of  $x$ ,  $n$  and  $k$ , and is shown in Table-8. It can be seen that the values obtained from computed values match well with the results obtained from correlation equations.

In general, to model the interstellar extinction, one need to execute the light scattering code with differ-

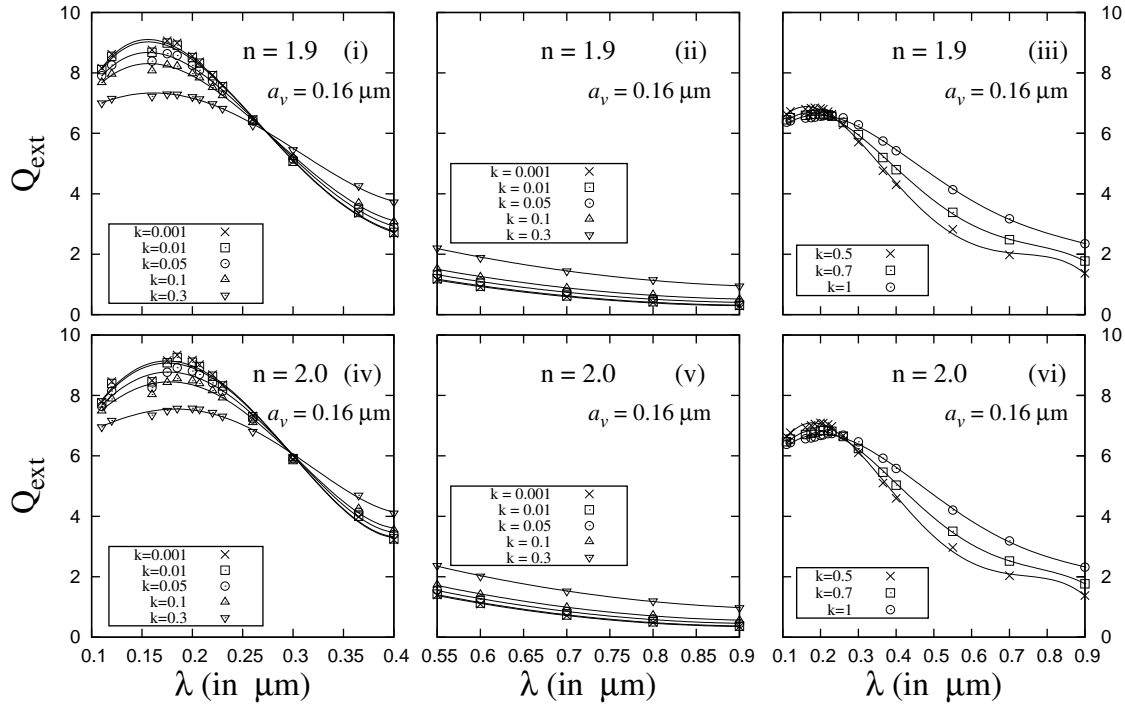


**Fig. 12** Same as Fig. 11 but with  $n = 1.9$  and  $2.0$ .

aggregates, it is possible to obtain the average extinction curves for silicate and graphite (and/or amorphous carbon) particles. With a suitable mixing among them, extinction curve against different wavelengths can be generated which can be fitted well with observed extinction curve. Some good pieces of work on modeling were already done for aggregate particles. Some preliminary results on modeling of interstellar extinction using aggregate dust model were already reported by [Bhattacharjee et al. \(2010\)](#). The present study shows that it is possible to study the extinction properties of interstellar dust aggregates for a given size of the particles and wavelength using relations (4), (5) and (6). The set of correlation equations can be used to estimate the general extinction  $A_\lambda$  using equation (1) for a given size distribution which will help to model the interstellar extinction curve. At this stage, we are not interested in modeling as this study is primarily projected to investigate the dependency of extinction efficiency on size, wavelength and composition of particles. We show how this dependency can be framed with some correlation equations to study the extinction properties of interstellar dust.

[Tamanai et al. \(2006\)](#) experimentally investigated the morphological effects on the extinction band in the infrared region for amorphous silica ( $\text{SiO}_2$ ) agglomerates. They also compared the measured band profiles with calculations for five cluster shapes applying Mie, T-matrix and DDA codes. Our correlations will be



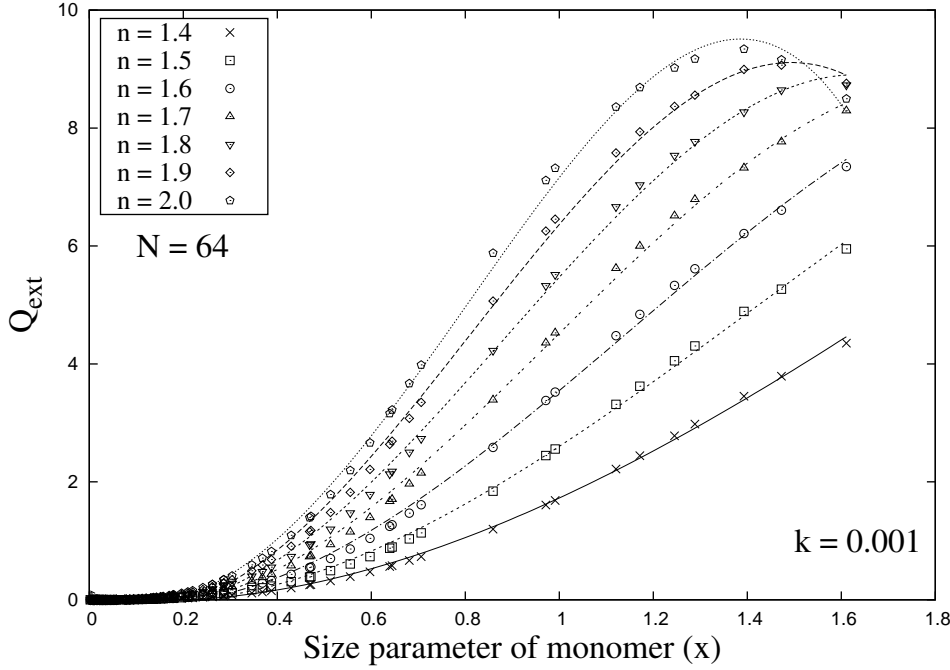


**Fig. 13** Extinction efficiency ( $Q_{ext}$ ) is plotted against the size parameter of monomer ( $x = 2\pi a_m/\lambda$ , where,  $0.01 \leq x \leq 1.6$ ) for  $N = 64$  and  $k = 0.001$ . The best fit curves represent a *cubic regression* for all values of  $n$  except 2.0, where a *quartic regression* (degree 4) is noticed. In all cases, the *coefficient of determination* ( $R^2$ )  $\approx 0.99$ .

parameter, composition etc.) of the experimental setup before using the correlation equations, because the relations are based on some selected set of parameters.

## 5 SUMMARY

1. We have first studied the dependency of  $Q_{ext}$  on size of the aggregates ( $a_m$ ) to investigate the correlations between  $Q_{ext}$  and complex refractive indices ( $n, k$ ) at a particular size. Computations are performed at four different sizes ( $a_v = 0.004, 0.068, 0.16$  and  $0.26 \mu m$ ).

If  $k$  is fixed at any value between 0.001 and 1.0,  $Q_{ext}$  increases with increase of  $n$  from 1.4 to 2.0.  $Q_{ext}$  and  $n$  are correlated via *linear regression* when the cluster size is small whereas the correlation is *quadratic* at moderate and higher sizes of cluster. This feature is observed at all wavelengths (UV to optical to infrared). We have also found that the variation of  $Q_{ext}$  with  $n$  is very small when  $\lambda$  is high. We have observed that  $Q_{ext}$  and  $k$  are correlated via polynomial regression equation (of degree 2, 3 or 4) where the degree of equation depends on the cluster size, real part of the refractive index of the particles ( $n$ ) and wavelength ( $\lambda$ ) of incident radiation. At  $a_v = 0.16 \mu m$ ,  $Q_{ext}$  and  $k$  is found to be correlated with a polynomial regression equation (of degree 2 or 3) when  $\lambda$  is between  $0.11 \mu m$  and  $0.26 \mu m$ . However, when  $\lambda > 0.26 \mu m$ , we have found that the correlation between them is *quadratic* for all values of  $n$ . The vertical range of  $Q_{ext}$  in the plot also decreases when  $k$  increases. This range is

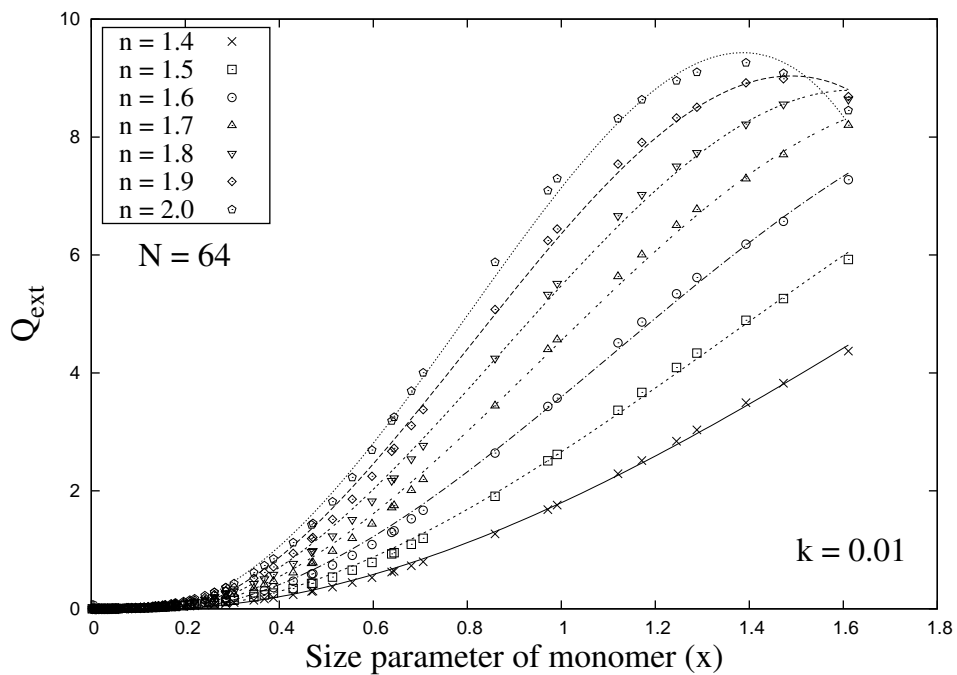


Fig. 14 Same as Fig.13 but with  $k = 0.01$ .

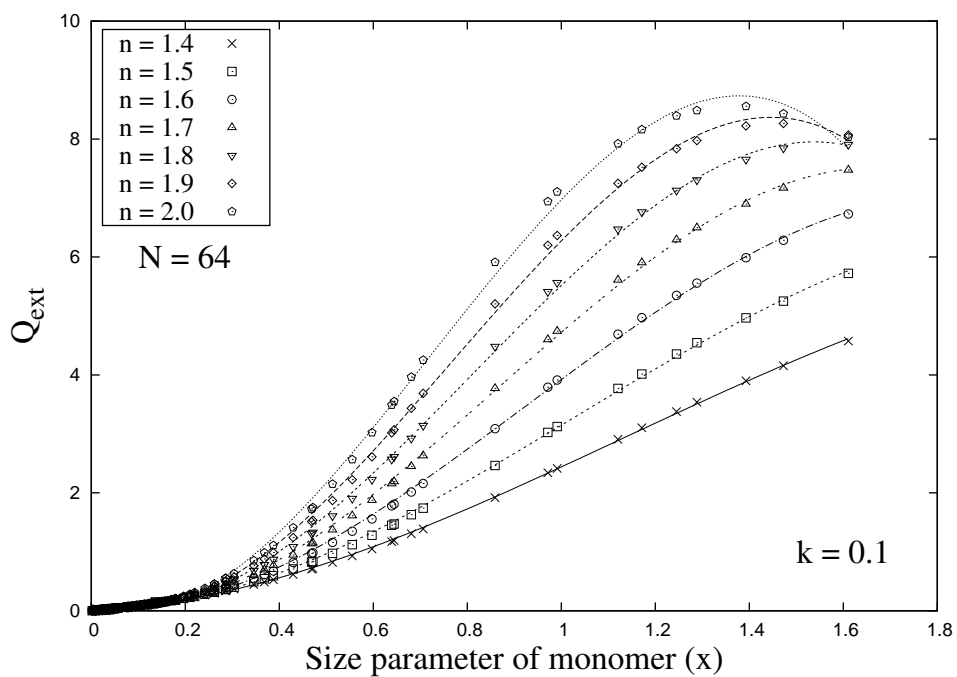
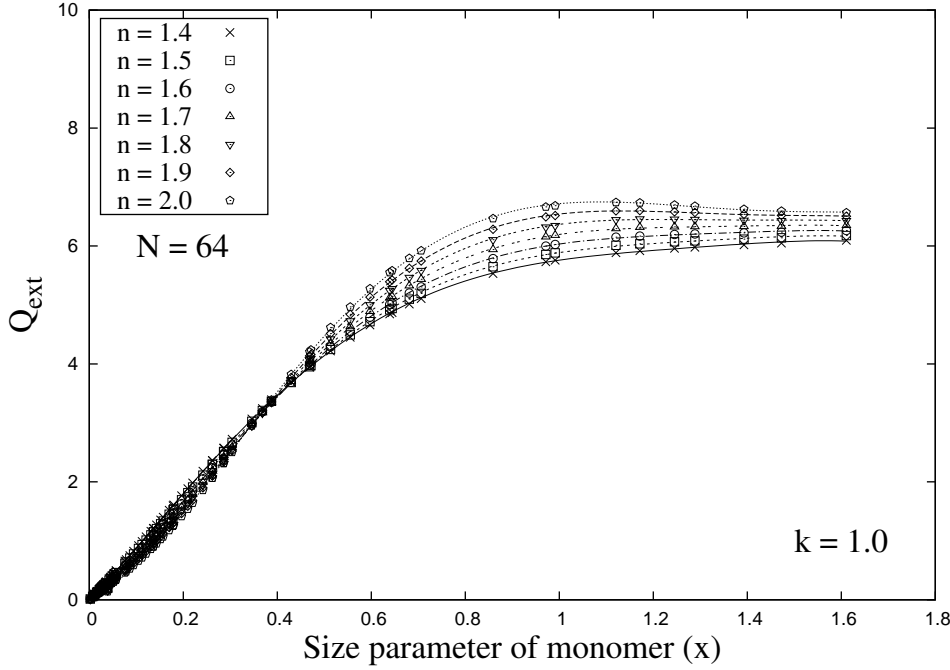


Fig. 15 Same as Fig.13 but with  $k = 0.1$ .

we can summarize that the correlation of  $Q_{ext}$  and  $k$  depends mainly on cluster size. The correlation is linear for small size and quadratic/cubic/quartic for moderate and higher sizes.

2. We study the dependence of  $Q_{ext}$  on  $\lambda$  for  $a_v = 0.16\mu m$ .  $Q_{ext}$  decreases with increase of  $\lambda$  when



**Fig. 16**  $Q_{ext}$  is plotted against  $x$  for  $N = 64$  and  $k = 1.0$ . In this case, the best fit curves correspond to a *quintic regression* (degree 5) for all values of  $n$ . Here,  $R^2 \approx 0.99$ .

it starts decreasing if  $\lambda$  is increased further. For  $n = 1.4, 1.5$  and  $1.6$ ,  $Q_{ext}$  versus  $\lambda$  can be fitted via a *quartic regression* for all values of  $k$ . For other values of  $n$ , the correlation is polynomial regression where the degree of equation depends on the value of  $n, k$  and  $\lambda$ .

3. We have found that  $Q_{ext}$  and  $x$  are correlated via a polynomial regression (of degree 3,4 or 5) for all values of  $n$ . The degree of regression is found to be  $n$  and  $k$ -dependent.
4. The correlation equations can be used to model interstellar extinction for dust aggregates in a wide range of size of the aggregates, wavelengths and complex refractive indices.

## 6 ACKNOWLEDGEMENT

We acknowledge Daniel Mackowski and Michael Mishchenko, who made their Multi-sphere T-matrix (MSTM) code publicly available. We also acknowledge Prithish Halder for help on the execution of JaSTA-2 software package. The reviewer of this paper is highly acknowledged for useful comments and suggestions.

## References

- Bhattacharjee C., Das H. S., Sen A. K., 2010, Assam University Journal of Science & Technology : Physical Sciences and Technology, 6 (Number II), 39
- Brownlee D. E., 1985, Ann. Rev. Earth Planet. Sci., 13, 147.
- Das H. S., Das S. R., Paul T., Suklabaidya A., Sen A.K, 2008, MNRAS, 389,787.
- Das H. K., Voshchinnikov N. V., Il'in V.B, MNRAS, 2010. 404, 265.

**Table 5** All co-efficient of equations (4), (5) and (6).

$k$	$n$	$\alpha_1$	$\alpha_2$	$\alpha_3$	$\alpha_4$		
0.001	1.4	-0.425	2.844	-0.728	0.034		
	1.5	-1.179	5.041	-1.316	0.056		
	1.6	-2.239	7.681	-1.976	0.082		
	1.7	-3.654	10.775	-2.712	0.109		
	1.8	-5.362	14.173	-3.475	0.136		
	1.9	-7.242	17.624	-4.175	0.158		
0.01	1.4	-0.502	2.931	-0.660	0.032		
	1.5	-1.248	5.085	-1.231	0.055		
	1.6	-2.312	7.713	-1.888	0.080		
	1.7	-3.714	10.772	-2.617	0.107		
	1.8	-5.367	14.060	-3.346	0.133		
	1.9	-7.189	17.404	-4.011	0.153		
0.1	1.4	-0.891	3.035	0.273	0.023		
	1.5	-1.588	4.882	-0.186	0.038		
	1.6	-2.540	7.120	-0.715	0.055		
	1.7	-3.726	9.652	-1.276	0.072		
	1.8	-5.100	12.358	-1.829	0.087		
	1.9	-6.569	15.046	-2.302	0.097		
$k$	$n$	$\beta_1$	$\beta_2$	$\beta_3$	$\beta_4$	$\beta_5$	
0.001	2.0	-2.164	-2.689	15.031	-3.120	0.102	
0.01	2.0	-1.926	-3.285	15.343	-3.097	0.103	
0.1	2.0	0.323	-8.985	18.392	-2.869	0.109	
$k$	$n$	$\gamma_1$	$\gamma_2$	$\gamma_3$	$\gamma_4$	$\gamma_5$	$\gamma_6$
1.0	1.4	-2.709	12.371	-18.540	6.182	8.466	-0.009
	1.5	-2.973	14.016	-22.167	9.438	7.576	-0.003
	1.6	-3.253	15.774	-26.024	12.846	6.686	0.005
	1.7	-3.540	17.603	-30.058	16.378	5.800	0.014
	1.8	-3.861	19.625	-34.440	20.118	4.901	0.024
	1.9	-4.222	21.861	-39.192	24.073	3.988	0.035
	2.0	-4.625	24.319	-44.317	28.233	3.061	0.047

Halder P., and Das H. S., 2017, Comp. Phy. Comm. (accepted, Article reference = COMPHY6306,

Corresponding author = H S Das)

Halder P., Chakraborty A., Deb Roy P. and Das H. S., 2014, Comp. Phy. Comm. 185, 2369

Iati M. A., Giusto A., Saija R., Borghese F., Denti P., Cecchi-Pestellini C. and Aiello S., 2004, ApJ, 615, 286.

Jones A. P., 1988, MNRAS, 234, 209.

Kimura H., 2001, JQSRT, 70, 581.

Krueger F. R. and Kissel J., 1989, Origins of Life and Evolution of the Biosphere, 19, 87

Mackowski D. W., and Mishchenko M. I., 1996, J. Quant. Spectrosc. Radiat. Transfer, 13, 2266.

Mathis J., Whiffen G, 1989, ApJ, 341, 808.

Mazarbhuiya, A. M. & Das, H. S., 2017, Astrophys Space Sci, 362, 161.

**Table 6**  $Q_{ext}$  for selected values of  $n$  and  $k$  from the relation (using equation (2)) and computations (from the simulations) where  $a_m = 0.041\mu m$  and  $0.11 \leq \lambda \leq 3.4\mu m$ . The difference between correlation equation and computed value is  $\text{Diff.} = |Q_{ext}(\text{corr}) - Q_{ext}(\text{comp})|$

$\lambda$	$n$	$k$	$Q_{ext}(\text{corr})$	$Q_{ext}(\text{comp})$	Diff.
0.11	1.5	0.001	7.487	7.555	0.068
	1.7	0.01	8.316	8.353	0.037
	1.9	0.1	7.729	7.683	0.046
0.20	1.5	0.001	4.368	4.305	0.063
	1.7	0.01	6.738	6.771	0.033
	1.9	0.1	7.963	7.975	0.012
0.30	1.5	0.001	1.881	1.842	0.039
	1.7	0.01	3.431	3.441	0.010
	1.9	0.1	5.179	5.205	0.026
0.40	1.5	0.001	0.906	0.895	0.011
	1.7	0.01	1.753	1.749	0.004
	1.9	0.1	3.057	3.070	0.013
0.55	1.5	0.001	0.390	0.388	0.002
	1.7	0.01	0.768	0.768	0.000
	1.9	0.1	1.513	1.513	0.000
0.70	1.5	0.001	0.205	0.203	0.002
	1.7	0.01	0.406	0.406	0.000
	1.9	0.1	0.879	0.880	0.001
0.90	1.5	0.001	0.103	0.102	0.001
	1.7	0.01	0.208	0.208	0.000
	1.9	0.1	0.508	0.509	0.001
3.4	1.5	0.001	0.002	0.002	0.001
	1.7	0.01	0.008	0.009	0.001
	1.9	0.1	0.056	0.056	0.001

Meakin P., 1984, Phys. Rev. A, 29,997.

Mukai T., Ishimoto H., Kozasa T., Blum J., Greenberg J. M., 1992, A&A, 262, 315.

Spitzer L., 1978, in Physical Processes in the Interstellar Medium. Wiley-Interscience Publication, New York.

Tamanai A., Mutschke H., Blum J., Neuhäuser R., 2006, JQSRT, 100, 373.

Vaidya D. B. and Gupta R., 1999, A&A, 348, 594.

Vaidya D. B., Gupta R., and Snow T.P., 2007, MNRAS, 379, 791.

Vaidya D. B. and Gupta R., 2009, J. Quant. Spectrosc. Radiat. Transfer, 110, 1726.

Voshchinnikov N.V., Il'in V.B., Henningth., Dovkova D.N., 2006, A&A, 445, 167.

Whittet D. C. B., 2003, in dust in the Galactic Environment, 76, 2nd edition (UK: IOP Publishing Ltd.).

Wolff M. J., Clayton G. C., Martin P. G., & Schulte-Ladbeck R. E., 1994, ApJ, 423, 412.

Wolff M. J., Clayton G. C., and Gibson S. J., 1998, ApJ, 503,815.

Wurm G., Blum J., 1998, Icarus, 132, 125.

**Table 7**  $Q_{ext}$  for selected values of  $n$  and  $k$  from the relation (using equation (3)) and computations (from the simulations) where  $a_m = 0.041\mu m$  and  $0.30 \leq \lambda \leq 3.4\mu m$ . The difference between correlation equation and computed value is  $\text{Diff.} = |Q_{ext}(\text{corr}) - Q_{ext}(\text{comp})|$

$\lambda$	$n$	$k$	$Q_{ext}(\text{corr})$	$Q_{ext}(\text{comp})$	Diff.
0.30	1.5	0.001	1.902	1.842	0.060
	1.7	0.01	3.438	3.441	0.003
	1.9	0.1	5.180	5.205	0.025
0.40	1.5	0.001	0.918	0.895	0.023
	1.7	0.01	1.760	1.749	0.011
	1.9	0.1	3.049	3.070	0.021
0.55	1.5	0.001	0.394	0.388	0.006
	1.7	0.01	0.770	0.768	0.002
	1.9	0.1	1.513	1.513	0.000
0.70	1.5	0.001	0.205	0.203	0.002
	1.7	0.01	0.407	0.406	0.001
	1.9	0.1	0.879	0.880	0.001
0.90	1.5	0.001	0.102	0.102	0.000
	1.7	0.01	0.208	0.208	0.000
	1.9	0.1	0.509	0.509	0.000
3.4	1.5	0.001	0.002	0.002	0.000
	1.7	0.01	0.008	0.009	0.001
	1.9	0.1	0.056	0.056	0.000

**Table 8**  $Q_{ext}$  for selected values of  $n$ ,  $k$  and  $x$  from the relation (using equations (4), (5) and (6)) and computations (from the simulations). The difference between correlation equation and computed value is  $\text{Diff.} = |Q_{ext}(\text{corr}) - Q_{ext}(\text{comp})|$

$x$	$n$	$k$	$Q_{ext}(\text{corr})$	$Q_{ext}(\text{comp})$	Diff.
0.286	1.5	0.001	0.064	0.092	0.028
0.286	1.7	0.01	0.152	0.207	0.055
0.286	1.9	0.1	0.514	0.506	0.008
0.468	1.5	0.001	0.424	0.388	0.036
0.468	1.7	0.01	0.862	0.768	0.094
0.468	2.0	1.0	4.183	4.205	0.022
0.706	1.5	0.001	1.225	1.136	0.089
0.706	1.9	0.1	3.660	3.688	0.028
0.706	2.0	0.1	4.169	4.252	0.083
0.972	1.5	0.001	2.459	2.446	0.013
0.972	1.7	0.01	4.333	4.397	0.064
0.972	2.0	1.0	6.693	6.664	0.029
1.171	1.5	0.001	3.534	3.622	0.088
1.171	1.9	0.1	7.485	7.522	0.037
1.171	2.0	1.0	6.728	6.733	0.005
1.289	1.5	0.001	4.208	4.305	0.097
1.289	1.7	0.01	6.674	6.771	0.097
1.289	1.9	0.1	8.058	7.975	0.083
1.473	1.5	0.001	5.287	5.268	0.019
1.473	1.7	0.01	7.754	7.702	0.052
1.473	1.9	0.1	8.357	8.264	0.093